Appl. Phys. A 84, 143–148 (2006)
DOI: 10.1007/s00339-006-3574-4

Applied Physics A
Materials Science & Processing

X.L. TONG✉
D.S. JIANG
W.B. HU
Z.M. LIU
M.Z. LUO

The comparison between CdS thin films grown on Si(111) substrate and quartz substrate by femtosecond pulsed laser deposition

Key Laboratory of Fiber Optic Sensing Technology and Information Processing
(Wuhan University of Technology), Ministry of Education, Wuhan 430070, P.R. China

Received: 30 January 2006/Accepted: 9 February 2006
Published online: 25 March 2006 •

ABSTRACT Two kinds of cadmium sulfate (CdS) thin films have been grown at 600 °C onto Si(111) and quartz substrates using femtosecond pulsed laser deposition (PLD). The influence of substrates on the structural and optical properties of the CdS thin films grown by femtosecond pulsed laser deposition have been studied. The CdS thin films were characterized by X-ray diffraction (XRD), atomic force microscopy (AFM), scanning electron microscopy (SEM), photoluminescence (PL) and Raman spectroscopy. Although CdS thin films deposited both on Si(111) and quartz substrates were polycrystalline and hexagonal as shown by the XRD , SEM and AFM results, the crystalline quality and optical properties were found to be different. The size of the grains for the CdS thin film grown on Si(111) substrate were observed to be larger than that of the CdS thin film grown on quartz substrate, and there is more microcrystalline perpendicularity of *c*-axis for the film deposited on the quartz substrate than that for the films deposited on the Si substrate. In addition, in the PL spectra, the excitonic peak is more intense and resolved for CdS film deposited on quartz than that for the CdS film deposited on Si(111) substrate. The LO and TO Raman peaks in the CdS films grown on Si(111) substrate and quartz substrate are different, which is due to higher stress and bigger grain size in the CdS film grown on Si(111) substrate, than that of the CdS film grown on the amorphous quartz substrate. All this suggests that the substrates have a significant effect on the structural and optical properties of thin CdS films.

PACS 81.15.Fg; 81.05.Ea; 78.20.-e; 78.67.-n; 42.62.-b

1 Introduction

Cadmium sulfide (CdS) is an important group II–VI semiconductor with a direct band gap of 2.48 eV at room temperature. Extensive research has been done in the last two decades on CdS thin films, mainly due to its applications in large area electronic devices like field-effect transistors, solar cells, photoconductors, optical thin film filters, nonlinear integrated optical devices, and light emitting diodes (LEDs) or laser heterostructures for emission in the visible spectral range [1–6]. CdS thin films have been grown by using various techniques, such as thermal evaporation (TE), chemical vapor deposition (CVD), metalorganic vapor-phase epitaxy (MOVPE), close space vapour transport (CSVT), chemical bath deposition (CBD), photochemical deposition (PD), rf sputtering (Sp), spray pyrolysis (SP), vapour transport deposition (VTD), screen printing (ScP), and electro deposition (ED). Besides various other techniques, pulsed laser deposition (PLD) has emerged as a technique for growing CdS thin films [7–9]. The main advantage of the PLD technique is its simplicity and low cost, and it is possible to obtain uniform films with good adherence and reproducibility. The PLD has many features such as that the laser target ablated by laser can create a highly energetic growth precursor, leading to formation of nonequilibrium growth conditions, so that high-quality films can be obtained at a fairly low substrate temperature [10]. Pulsed laser deposition has become an appealing growth technique of CdS thin films. For this growth method, lasers in the nanosecond temporal regime have been used commonly, i.e., nanosecond pulsed excimer and Q-switched Nd:YAG lasers [11–13]. Recently, studies have been reported in the literature, concerning the growth of nitride thin films and oxide thin films and so on by femtosecond PLD [14, 15]. However, there is little in the current literature on CdS thin films formed by a femtosecond PLD. Femtosecond lasers emit light at very high intensities (up to 10^{21} W/cm^2) and short pulse widths (10^{-14} to 10^{-15} s).

It is assumed that when the laser pulse temporal length become shorter than the time needed to couple the electronic energy to the lattice, i.e., a few picoseconds, thermal effects can not play a significant role. Moreover, the multiphoton absorption process which was very likely to occur at high laser intensities currently reached with femtosecond lasers, should also overcome the problem of a too low optical absorption coefficient in wide band gap (good insulators) materials [15]. The femtosecond PLD utilizes a short-pulse high-energetic laser beam to ablate material from a target and deposit this material onto a substrate placed in a vacuum chamber. Stress and adhesion determine the quality of a thin film/substrate composite. The structural and optical properties of thin CdS films can be influenced by the substrate on which it is deposited. In fact, the substrate affects the deposition process by directly determining strains due to lattice and thermal expansion mismatch. Comparison of the structural and optical properties of thin CdS films deposited on Si(111) and quartz

✉ Fax: +86-27-87665287, E-mail: tongxinglin@263.net

substrates is very helpful in selecting the substrate for useful devices based on CdS structures. It is fairly difficult to grow a film of high quality with a smooth surface free from cracks, because of the large lattice mismatch and the large thermal expansion coefficient mismatch between the grown film and substrate. In particular, very little is known about the role of substrates on films growth. With this as its aim, in this paper we present the growth of CdS films on silicon and quartz substrates by femtosecond pulsed laser deposition, we report a study of the influence of Si(111) and quartz substrates on the structural and optical properties of the thin CdS films.

2 Experimental

Although the substrate temperature and the laser fluence were the important parameters for CdS thin films grown by femtosecond PLD, in order to compare the effects of the Si(111) and quartz substrates on the structural and optical properties of the CdS films, we do not discuss the effects of the substrate temperature and the laser fluence in the paper. The experimental process is thus as follows below.

Two samples of CdS thin films was prepared by femtosecond PLD onto Si(111) and quartz substrates, respectively. The femtosecond PLD experiments have been realized in a standard PLD configuration consisting of laser systems, a deposition chamber, a CdS target and a substrate. The details of the deposition chamber have been described previously [10]. In the experiment, the deposition was carried out in a stainless steel vacuum chamber evacuated by a turbomolecular pump to a base pressure of 10^{-3} Pa. A femtosecond pulsed Ti:sapphire laser (Spectra Physics, Spitfire 50 fs) was used for the experiments. This system was comprised of a pulse stretcher, a regenerative amplifier that was pumped by an Nd:YLF laser, and a compressor. The laser emits 90 fs pulses at a central wavelength of 800 nm (photon energy 1.55 eV). The nominal beam diameter was 8 mm. In the experiments, the laser was operated in continuous shot mode at a pulse frequency of 1 kHz. The femtosecond laser was focused by a lens on a rotating CdS (99.999%) target. The Si(111) and quartz substrates were simultaneously placed around 4 cm from the target and parallel to it on a rotating holder. During the deposition process, the laser fluence and substrate temperature were 1.2 J/cm^2 and 600 °C, respectively. For the two samples of CdS thin films deposited onto the Si(111) and quartz substrates, the deposition time was 10 min. The thickness of the two CdS thin films was measured using an ellipsometer, and the thickness of the resulting films are approximately the same, which is about 500 nm. The structural and optical properties between the two kinds of thin films were compared and analyzed by X-ray diffraction (XRD), atomic force microscopy (AFM), scanning electron microscopy (SEM), photoluminescence (PL) and Raman spectroscopy, respectively.

In order to examine the crystalline structure and orientation of the CdS thin films, high-resolution X-ray diffraction (XRD) was used to characterize the phases in the CdS thin films. The X-ray diffraction (XRD) measurements were performed on a Philips X'Pert X-ray diffractometer using a Cu $K_{\alpha 1}$ source ($\lambda = 1.5406$ Å) and a thin film attachment. We used the grazing angle X-ray diffraction technique here to ensure that the diffraction patterns originate mainly from the thin films and not its substrates. The surface morphology and grains size of the CdS thin films were examined by atomic force microscopy (AFM, DI Nanoscope IV SPM) and scanning electron microscopy (SEM, Sirion 200 FEI). The photoluminescence measurements were performed with the cw emission at 325 nm of a He-Cd laser with an intensity of 3 W/cm^2. Raman spectra were recorded by using the unpolarized Raman measurements. Raman spectra were recorded by means of a Raman confocal microspectrometer apparatus, using the 633 nm line of a He-Ne laser and a notch filter (200 cm^{-1} line-width) to suppress the scattered laser light. All these characterization measurements were carried out at room temperature.

3 Results and discussion

3.1 *The crystalline quality of the* CdS *thin films*

Figure 1a–b show the XRD measurements results of the two CdS thin films samples grown onto Si(111) and quartz substrates using femtosecond PLD under the same experimental conditions. As can be seen from Fig. 1a-b, the CdS films grown on Si(111) and quartz substrates exhibit nine obvious CdS peaks in the diffraction pattern. The XRD peaks which are located at $2\theta = 24.9°$, 26.6°, 28.2°, 36.7°, 43.8°, 48.0°, 52.0°, 54.5° and 67.1° are attributed to CdS(100), CdS(002), CdS(101), CdS(102), CdS(110), CdS(103), CdS(112), CdS(004), and CdS(203), respectively. The XRD results reveal that the two CdS films samples deposited by femtosecond PLD are polycrystalline. However, the crystalline quality of the two CdS films samples is not as good as that of films grown using a nanosecond laseras reportedin the literature [13]. It is related to the dynamic expansion of the plasma plume induced by femtosecond pulses, which generates high-kinetic energy species. When the smaller molecular fragments reach the substrate surface,

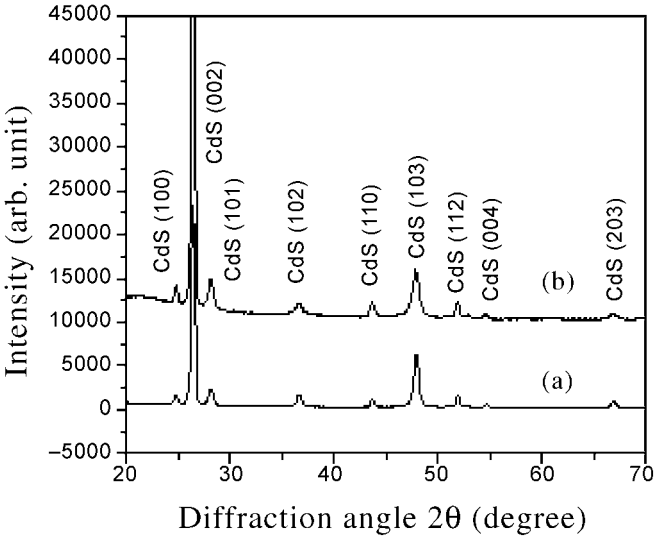

FIGURE 1 XRD measurements results of the CdS films grown on Si(111) substrate (**a**) and quartz substrate (**b**)

they have not enough time to grow in a preferential direction, so that they are overlaid and solidified by the follow-up species. Therefore, a comparatively poor polycrystalline thin film is formed by femtosecond PLD. As can be seen, both the two CdS films samples have hexagonal structures and the main reflections were the hexagonal (002) and (103). The (002) reflection is the most intensive. This resultshows that the microcrystalline parallelism of the *c*-axis in the films is preferential. In addition, the second strongest peak is the (103) peak. Compared to the (103) peak of the CdS film grown on the Si(111) substrate in Fig. 1a, the (103) peak of the CdS film grown on quartz substrate in Fig. 1b is obviously enhanced. This reveals that there is more microcrystalline perpendicularity of the *c*-axis in the films deposited on the quartz substrate than that in the films deposited on the Si substrate. The above differences may be attributed to the orientation on the substrate, which is caused by the variations of the plume on different substrates. The clusters included in the very high anisotropy of the plume in femtosecond laser ablation would be the deposition, in which the substrates are covered by the films. The films stick to the largest and smoothest area, i.e., with the cleavage, on the surface of the substrate. The clusters on the substrate melt and re-crystallize at the film surface due to the high temperature prevailing during laser ablation differences of the substrates. This causes variation of the interatomic spacing with crystal size, recrystallization processes, microscopic voids and special arrangements of dislocation and phase transformations. Since the cleavages are parallel and perpendicular to the *c*-axis, the films grow with parallel and perpendicular orientation to the substrate surface.

3.2 *The morphologies of the* CdS *thin films*

3.2.1 The SEM of the CdS *thin films.* Figure 2a–b show scanning electron micrographs of the CdS films grown on Si(111) and quartz substrates. As can be seen from the figure, the films seem to be composed of granules. There is no droplet observed, which is generally assumed to be the consequence of thermal effects during the laser-matter, liquid material being ejected as droplets from the molten zone of an irradiated target. And droplets are generally observed in the films grown by nanosecond PLD. In fact, the high intensity available with femtosecond lasers, leads to multiphoton absorption, while the use of femtosecond pulse lasers will limit the thermal diffusion and its corresponding effects inside the CdS target. Femtosecond pulse energy is absorbed in the near vicinity of the CdS target surface, leading to high ionization of the ablation populations of species (ions, neutrals and clusters) deposited on substrates. The growth of CdS films by fs PLD has shown that the two CdS film samples consist of stacked nanocrystallites and present a polycrystalline film. The SEM image shows that such random stacking of spherical particles was also observed for the films grown either on Si or quartz substrates. It suggested the substrate as a possible origin of cluster formation. However, the CdS films grown on Si(111) substrate also show particles but on a larger scale than observed for the CdS films grown on quartz substrate. It could be deduced that more nuclei were generated for the CdS grown on amorphous quartz substrate when the plasma reaches the substrate surface than that for the CdS grown on unit-cell silicon.

3.2.2 The AFM of the CdS *thin films.* The corresponding AFM images of the two CdS film samples surface topography are shown in Fig. 3a–b. All the images were obtained in tapping mode with standard Si tips of radius 10 nm. The images were post-processed using a quadratic plane fit in both directions, in some cases, a zero-order line-by-line flattening routine, and Fig. 3a–b was measured by AFM over $5 \times 5\ \mu m^2$ scanning ranges. The growth of the grain size due to substrates is clearly seen from a comparison of images Fig. 3a–b. One can identify that the films are constructed in the columnar shape and the surface grain size corresponds to the actual grain size. While both films appear as dense aggregates of independent nanoparticles, a clear difference in the grains size in the two cases can be observed, namely, the average size of particles of CdS thin films grown on Si and quartz substrates is 74.9 and 48.8 nm, respectively. When the flow of ablated species impinges on the substrate, the deposit is mainly due to the aggregation of CdS clusters leading to a heterogeneous growth. Initially, the growth is via the three-dimensional mode. The islands formed on the substrates surface start to coalescence and new small islands start to grow between the bigger islands. A certain thickness of the films are formed, which transform the growth mode into the pseudo-two-dimensional grow, and therefore leads to a high surface roughness. The surface root-mean square roughness values for the CdS thin films grown on Si and quartz substrates

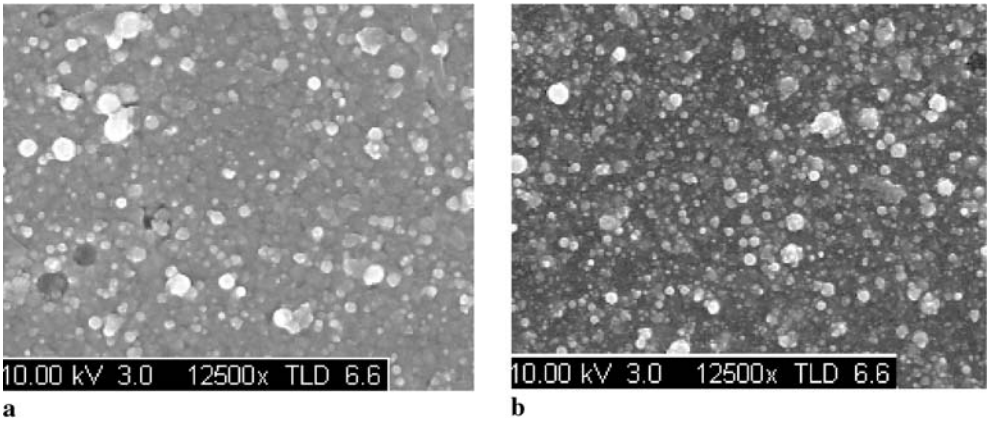

a **b**

FIGURE 2 SEM micrograph of the CdS films grown on Si(111) substrate (**a**) and quartz substrate (**b**)

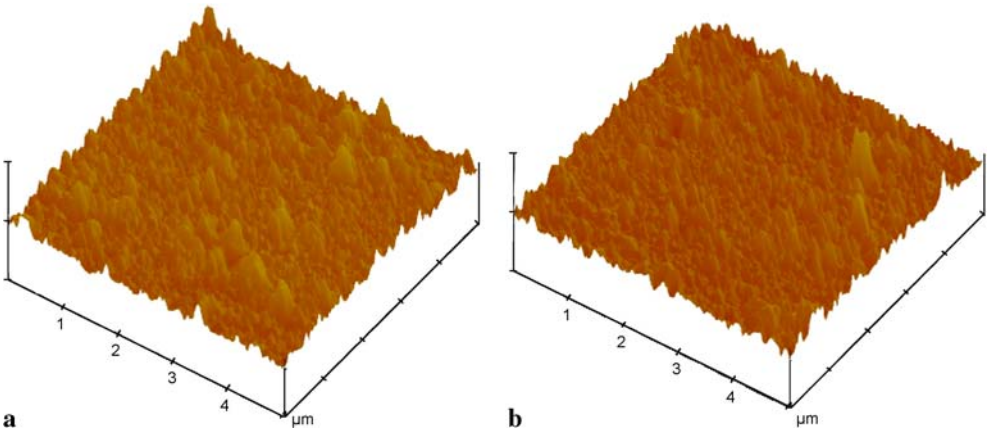

FIGURE 3 Surface three-dimensional topography of the CdS films grown on Si(111) substrate (**a**) and quartz substrate (**b**)

were determined to be 21.9 and 20.8 nm, respectively. From the AFM measurements one could conclude, that the CdS thin film grown on Si substrate is slightly rougher than the CdS thin films grown on quartz substrate. The rough surface systematically observed on the deposits is not the result of droplets directly transferred from the CdS target, but is due to the formation of aggregated particles. For the different substrate, the average size of grains and agglomerated particles are also different, therefore, the surface roughness of the CdS thin films grown on Si and quartz substrates is different.

3.3 *Photoluminescence analysis*

PL spectra of the two CdS film samples are shown in Fig. 4a and b, respectively. The broad weak emission peak for the two CdS thin films samples is a result of poor polycrystalline quality and some defects on the surface of the CdS thin films. Each PL spectrum is characterized by two emission weak bands. A blue band emission with a peak centered at around 445 nm, which can be attributed to excitonic transitions. The absence of excitions is probably caused by electric fields between the microcrystallites of thin film CdS [16]. Typically, in semiconductors like CdS, excitonic peak appears at energies lower (wave lengths larger than 500 nm) than the band gap energy (2.48 eV). However, as shown in Fig. 4a–b, the maximum emission peak blue-shifts from 500 to 445 nm. A possible explanation for the band at 445 nm is that it is related to the confinement effects and the direct inversion of the fundamental absorption edge for the nanometric dimensions of the crystallite [4]. The other green band composed of a peak centered at around 520 nm, originated from radiative recombination [17], which was related to the grain size distribution. The excitonic peak is more intense and resolved for CdS deposited on quartz with respect to the films deposited on Si(111) substrate. Such a result suggests that the CdS thin film grown on quartz substrate has better optical properties than the CdS thin film grown on Si(111) substrate. From the PL analysis the quartz substrate seems to have a better matching with the deposited films, as demonstrated by the higher radiative efficiency at room temperature of the film grown on quartz substrate with respect to those grown on Si(111) substrate.

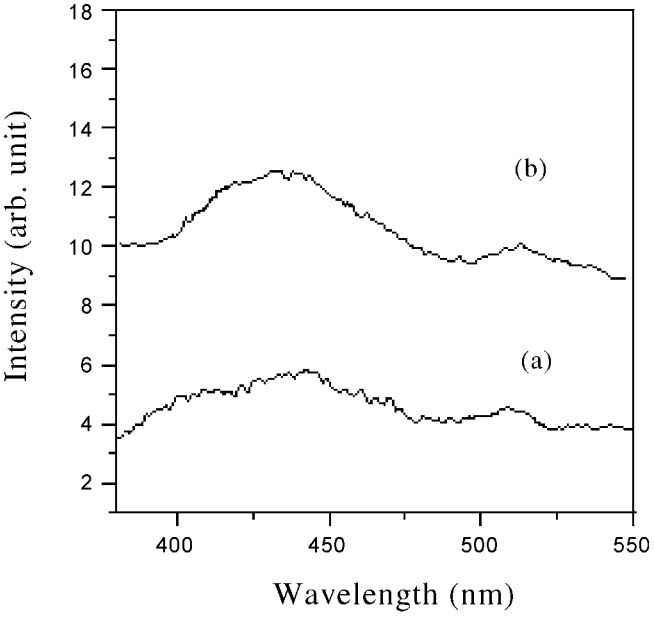

FIGURE 4 Photoluminescence spectra of the CdS films grown on Si(111) substrate (**a**) and quartz substrate (**b**)

The green band peak at 520 nm was probably due to recombination at surface grains. Formation of CdS nanoparticles is a result of film–substrate interaction due to molecular forces acting at the interface of three-dimensional islands, since the nanoparticles are probably nucleated at and remain in contact with the pore walls. The green band peak intensity is larger for the film grown on quartz substrate than that of the film grown on Si substrate. As the size of the grains was decreased, the ratio of surface to volume of the grain was increased and thus led to enhancement of the green band intensity, which may be explained by the fact that more Cd interstitials were trapped on the grain boundaries due to the increase of the surface-to-volume ratio of the grain as the grain size was decreased. This is because the films were preferentially formed by clusters, which causes grain boundaries during the film deposition. The grain size for the thin film grown on quartz substrate was considerably smaller. These grain boundaries give rise to the formation of radiative recombination centers within the green bandgap of the PL peaks [18]. These are in good agreement with the results from the AFM measurement of the CdS films.

3.4 *Raman spectra*

The room temperature Raman spectra of the two CdS films samples were acquired in unpolarization configuration. The Raman signals of the Si substrate, quartz substrate, as well as the CdS Raman peaks, are shown in Fig. 5a–b. The Raman feature peak centered on the *n*-type Si substrate is at approximately 520 cm^{-1}. The Raman feature peaks centered on the quartz substrate are at 476 cm^{-1} and 602 cm^{-1}. The Raman spectra for the CdS grown on Si is shown in Fig. 5a. Four CdS Raman peaks can be discerned, these are 1LO around 304 cm^{-1}, 2TO around 440 cm^{-1}, 2LO around 609 cm^{-1} and 3TO around 660 cm^{-1}. The corresponding full width at half maximum (FWHM) of the Raman peaks is 15 cm^{-1}, 9 cm^{-1}, 12 cm^{-1} and 14 cm^{-1}, respectively. Figure 5b shows Raman spectra of the CdS grown on quartz substrate. Four CdS Raman peaks can be discerned, these are 1TO around 214 cm^{-1}, 1LO around 300 cm^{-1}, 2TO around 428 cm^{-1} and 2LO around 600 cm^{-1}. And the corresponding full width at half maximum (FWHM) of the Raman peaks is 13 cm^{-1}, 25 cm^{-1}, 34 cm^{-1} and 14 cm^{-1}, respectively. In Fig. 5a, the phenomenon of the disappearance of the scattering intensity of the 1TO mode might be that the Raman signal of the 1TO mode is masked by the envelope of the 1LO signal. The different number of observable overtones is due to the resonant effect of the scattered Raman signal with exciton energy. The small number of overtones observed in the present study is due to our sample being a polycrystalline film. For the hexagonal CdS, there are LO (longitudinal optical) phonons which polarize along the z direction parallel to the unit cell edge, and TO (transverse optical) phonons which polarize along the direction parallel to the xy plane (normal to z direction). The frequencies of 1LO and 1TO of bulk CdS are known to be 305, 228 cm^{-1}, respectively [19]. In this presented work, the down-frequency shift of the 1LO Raman peak and the degraded TO phonon line in CdS thin film are mainly ascribed to the grain-size and stress effects [20], which change the vibrational characteristics of CdS thin films, leading to the shift of Raman frequency. The full width at half maximum (FWHM) of the Raman peaks of the CdS films grown on Si(111) substrate are smaller and the peak intensities are higher than that the CdS films grown on Si(111) quartz substrate. We can conclude that the Raman peaks intensity of CdS thin films might be mostly relative to the grains size. This low-frequency shift of the 1LO Raman peak in CdS thin film is mainly ascribed to the grain-size effect. Hence, the low-frequency shift of the corresponding LO Raman peak in the CdS films grown on Si(111) substrate is larger than that of the CdS films grown on quartz substrate. In addition, because the deformation potential is the main mechanism of TO mode scattering it can only be degraded. The deformation potential can be caused by the lattice mismatch and thermal expansion coefficient mismatch between the CdS films and the substrates. The TO peaks for the CdS films grown on Si(111) substrate have a blue shift which correspond to the TO peaks in the CdS films grown on quartz substrate. It can be inferred that this it is due to higher stress in the CdS film grown on Si(111) substrate than for that the CdS film grown on the amorphous quartz substrate.

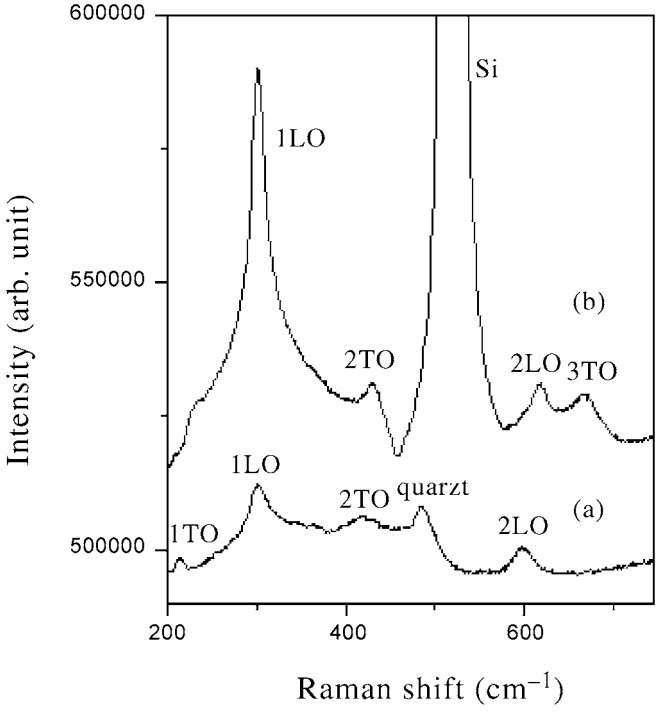

FIGURE 5 Raman spectra of the CdS films grown on Si(111) substrate (**a**) and quartz substrate (**b**)

4 Conclusions

A study have been carried out to investigate the structural and optical characterizations of CdS thin films deposited on Si(111) and quartz substrates using femtosecond pulsed laser deposition. We have demonstrated that the crystallinity, the surface quality and the optical character of the CdS thin films are related to the substrates. In summary, the two CdS films deposited by femtosecond PLD are polycrystalline, while the as-deposited films have a hexagonal mixed phase. Compared to the CdS film grown on Si(111) substrate, the grain size for the CdS thin films grown on quartz substrate was considerably smaller. In addition the CdS thin films grown on quartz substrate have better optical properties than the CdS films grown on Si substrate, which could be the result of the interaction between the CdS nanocrystallite and the substrates.

ACKNOWLEDGEMENTS This work is supported by the Postdoctoral Science Foundation of China (2005037666) and the Key Project of National Nature Science Foundation of China (60537050). This work, picked out as the best postdoctoral science and technology activity, is aided financially by the Hubei provincial government. The authors would like to acknowledge professor P.X. Lu, Y.B. Xu and Miss H. Long for the benefits from using the femtosecond laser device of the Wuhan National Laboratory for Optoelectronics in HUST.

REFERENCES

1 O. Trujillo, R. Moss, K.D. Vuong, D.H. Lee, R. Noble, D. Finnigan, S. Orloff, E. Tenpas, C. Park, J. Fagan, X.W. Wang, Thin Solid Films **290–291**, 13 (1996)
2 C.M. Dai, L. Horng, W.F. Hsieh, Y.T. Shih, J. Vac. Sci. Technol. A **10**, 484 (1992)
3 A. Morales-Acevedo, O. Vigil-Galán, G. Contreras-Puente, J. Vidal-Larrmendi, G. Arriaga-Mejia, M. Chavarria-Castafieda, A. Escamilla-Esquive, H. Hemández-Contreras, A. Arias-Carbajal, F. Cruz-Gandarilla,

Conference Record of the IEEE Photovoltaic Specialists Conference (2002), p. 624
4 B. Ullrich, D.M. Bagnall, H. Sakai, Y. Segawa, J. Luminesc. **87–89**, 1162 (2000)
5 G. Perna, V. Capozzi, S. Pagliara, M. Ambrico, D. Lojacono, Thin Solid Films **387**, 208 (2001)
6 J.A. Chediak, Z. Luo, J. Seo, N. Cheung, L.P. Lee, T.D. Sands, Sens. Actuators A **111**, 1 (2004)
7 B. Ullrich, R. Schroeder, IEEE J. Quantum Electron. **QE-37**, (2001) 1363
8 H. Wang, Y. Zhu, P.P. Ong, J. Cryst. Growth **220**, 554 (2000)
9 M. Khanlary, P. Townsenda, B. Ullrich, D.E. Hole, J. Appl. Phys. **97**, 023 512 (2005)
10 X.L. Tong, Q.G. Zheng, S.L. Hu, Y.X. Qin, Z.H. Ding, Appl. Phys. A **79**, 1959 (2004)
11 A. Erlacher, H. Miller, B. Ullrich, J. Appl. Phys. **95**, 2927 (2004)
12 G. Perna, V. Capozzi, M. Ambrico, V. Augelli, T. Ligonzo, A. Minafra, L. Schiavulli, M. Pallara, Thin Solid Films **453–454**, 187 (2004)
13 B. Ullrich, H. Sakai, Y. Segawa, Thin Solid Films **385**, 220 (2001)
14 M. Womack, M. Vendan, P. Molian, Appl. Surf. Sci. **221**, 99 (2004)
15 J. Perriére, E. Millon, W. Seiler, C. Boulmer-Leborgne, V. Craciun, O. Albert, J.C. Loulergue, J. Etchepare, J. Appl. Phys. **91**, 690 (2002)
16 Y. Yang, J.L. Shi, S.G. Dai, X.G. Zhao, X.H. Wang, Thin Solid Films **437**, 217 (2003)
17 A. Giardini, M. Ambrico, D. Smaldone, R. Martino, V. Capozzi, G. Perna, G.F. Lorusso, Mater. Sci. Eng. B **43**, 102 (1997)
18 C.T. Tsai, D.S. Chuu, G.L. Chen, S.L. Yang, J. Appl. Phys. **79**, 9106 (1996)
19 J. Lee, T. Tsakalakos, Nanostruct. Mater. **8**, 381 (1997)
20 D.S. Chuu, C.M. Dai, Phys. Rev. B **45**, 11 805 (1992)